REPORT DOCUMENTATION PAGE

Form Approved
OMB No. 0704-0188

1. REPORT DATE *(DD-MM-YYYY)*	**2. REPORT TYPE**	**3. DATES COVERED** *(From - To)*
May 2012	Technical Paper	May 2012-July 2012

4. TITLE AND SUBTITLE
Wind Compensation by Radiometer Arrays in High Altitude Propulsion

5a. CONTRACT NUMBER
In-House

5b. GRANT NUMBER

5c. PROGRAM ELEMENT NUMBER

6. AUTHOR(S)
Natalia Gimelshein, Sergey Gimelshein, Andrew Ketsdever, Marcus Young

5d. PROJECT NUMBER

5e. TASK NUMBER

5f. WORK UNIT NUMBER
50260542

7. PERFORMING ORGANIZATION NAME(S) AND ADDRESS(ES)

Air Force Research Laboratory (AFMC)
AFRL/RQRC
10 E. Saturn Blvd.
Edwards AFB CA 93524-7680

8. PERFORMING ORGANIZATION REPORT NO.

9. SPONSORING / MONITORING AGENCY NAME(S) AND ADDRESS(ES)
Air Force Research Laboratory (AFMC)
AFRL/RQR
5 Pollux Drive
Edwards AFB CA 93524-7048

10. SPONSOR/MONITOR'S ACRONYM(S)

11. SPONSOR/MONITOR'S REPORT NUMBER(S)
AFRL-RZ-ED-TP-2012-217

12. DISTRIBUTION / AVAILABILITY STATEMENT
Distribution A: Approved for Public Release; Distribution Unlimited. PA#12506

13. SUPPLEMENTARY NOTES
Conference paper for the International Symposium on Rarefied Gas Dynamics, Zaragoza, Spain, 09-13 July 2012.

14. ABSTRACT
Numerical analysis has been conducted to assess the feasibility of using radiometer arrays mounted on a near-space vehicle, for wind disturbance compensation. The results indicate the possibility of using radiometric force for that purpose for altitudes of 80 km and smaller, and head winds up to 30 m/s.

15. SUBJECT TERMS

16. SECURITY CLASSIFICATION OF:			**17. LIMITATION OF ABSTRACT**	**18. NUMBER OF PAGES**	**19a. NAME OF RESPONSIBLE PERSON**
					Marcus Young
a. REPORT	**b. ABSTRACT**	**c. THIS PAGE**			**19b. TELEPHONE NO** *(include area code)*
Unclassified	**Unclassified**	**Unclassified**	SAR	9	661-275-5624

Standard Form 298 (Rev. 8-98)
Prescribed by ANSI Std. 239.18

Wind compensation by radiometer arrays in high altitude propulsion

Natalia Gimelshein*, Sergey Gimelshein*, Andrew Ketsdever† and Marcus Young†

*ERC, Inc., Edwards AFB, CA 9352
†Propulsion Directorate, Edwards AFB, CA 93524

Abstract. Numerical analysis has been conducted to assess the feasibility of using radiometer arrays mounted on a near-space vehicle, for wind disturbance compensation. The results indicate the possibility of using radiometric force for that purpose for altitudes of 80 km and smaller, and head winds up to 30 m/s.

Keywords: Radiometers, kinetic methods, high altitude propulsion
PACS: 51.10.+y,47.45.-n, 07.60.Dq

INTRODUCTION

It is well known from the kinetic gas theory that there is a force resulting from nonequilibirium temperature gradients in a fluid. This force on a surface, usually called radiometric, and sometimes Knudsen force, is only observable in a thermally driven gas flow rarefied enough to have the local gas mean free path comparable to the characteristic size of the flow. This makes radiometric forces important in various low density environments as well as micro- and nano-scale systems. The radiometric forces may generally be created by various sources such as radiation or resistive heating, and the relative simplicity of producing and observing the effects of radiometric forces appears to be the main reason for the early discovery of the forces in 1825 by Fresnel [1], followed by the detailed analysis in the late 19th and early 20th centuries by a number of prominent scientists, including Crookes, Maxwell, Reynolds, Einstein, and others [2, 4, 3, 5].

Interest in radiometric phenomena, diminished after 1920s, started to grow rapidly in the last decade, primarily because the radiometric phenomena were found to be useful in a number of different micro- and large scale devices. One of the most notable of these is atomic force microscopy (AFM) [6], where the temperature of a cantilever can increase due to resistive heating under piezoelectic excitation or due to heating by a laser that senses the cantilever displacement, and an associated radiometric force is generated by thermally-induced rarefied gas flow. The radiometric force was also studied in application to modern microactuators [7], where the direct simulation Monte Carlo (DSMC) method was used to model forces on vanes mounted on an armature. More recently, Passian with co-workers have examined radiometric phenomena applied to microcantilevers both experimentally and analytically [8, 9]). At the other end of the length scale, a concept of a high-altitude aircraft supported by microwave energy that uses radiometric effects has been put forward in [10].

A near-space propulsion system using radiometric forces has recently been developed [11] for a generic near space vehicle. The purpose of the propulsion system, schematically illustrated in Fig. 1, is to provide wind disturbance compensation for the vehicle operating at an altitude range of 40 to 80 km. The system consists of an array of multiple square radiometer vanes integrated along the surface of a generic near-space vehicle. The trends obtained in the experimental and numerical analysis illustrated the feasibility of the design concept, and indicated the possibility to improve the radiometer system efficiency through the increase in height of individual vanes and optimizing the separation between the vanes. An important factor that was not accounted for in the previous work is the impact of finite free stream velocity on the output of radiometric system. The main objective of this work is the numerical analysis of radiometric forces on an array of small vanes installed on a near-space vehicle operating at altitudes between 60 and 80 km, with head winds varying from 0 to hundreds of meters per second.

The flow over a near-space vehicle at these altitudes is near continuum, and the flow velocity is expected to decrease from its free stream value in the far field to meters or even centimeters per second near the wall. To analyze the effect of the flow velocity in the vicinity of radiometer vanes on the radiometric force produced by the vane, a series of computations is performed for a single stand-alone vane immersed in a moving rarefied flow. After that, a two-step

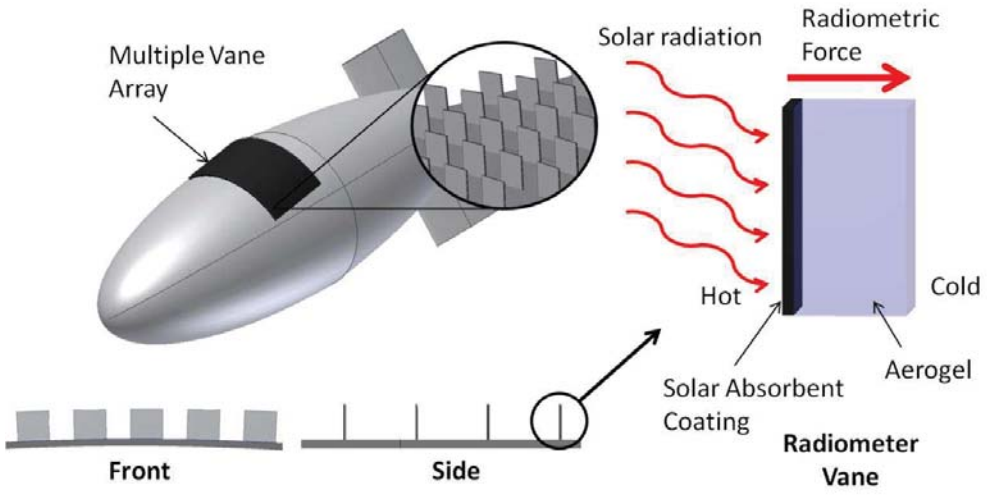

FIGURE 1. Concept of a near-space radiometric propulsion system.

approach is used to analyze the radiometric force from a large array of radiometers installed on a vehicle surface. The first step is the simulation of the entire flow over a model near-space vehicle, and the second step is the computation of a flow over a radiometer array using the boundary conditions extracted from the first-step solutions.

NUMERICAL APPROACH

Previous studies have shown that the radiometric force over a single vane reaches its maximum for a Knudsen number of about 0.1, and thus a quantitative analysis of radiometric forces requires a kinetic approach to be used. In this work, a kinetic solver SMOKE [13] is used, based on the solution of the Ellipsoidal Statistical kinetic equation. SMOKE is a parallel 2D/axisymmetric finite volume solver for model kinetic equations, based on conservative numerical schemes developed in [12]. SMOKE is used here to calculate the flow over a stand-alone vane and an array of radiometers installed on a surface of a near-space vehicle. A second order spatial discretization with is used along with implicit time integration.

Prescribed inflow boundary conditions are imposed for a stand-alone vane, with the computational domain chosen large enough to minimize the effect of the inflow boundaries. The diffuse model with complete energy and momentum accommodation is used for gas-surface interaction, and axial symmetry is applied at Y=0. The spatial grid typically consists of about 10,000 cells, and the velocity grid contains (20,18,18) (x, r, θ) points. The space and velocity convergence studies were conducted in earlier studies [14] where radiometric flows with similar Knudsen numbers were examined. To simulate a large array of tightly spaced radiometers installed on a space vehicle, calculations were conducted in a two-dimensional configuration for a single vane with periodic boundary conditions at the left and right boundaries, wall boundary conditions and the bottom boundary, and prescribed inflow boundary conditions at the top boundary. For the inflow conditions, the gas properties were taken from the computations of a flow over the entire space vehicle.

A Navier-Stokes solver CFD++ [15] is used to compute the flow over a space vehicle, which in this work is modeled as a 2 m thick and 10 m long ellipsoid. The thickness-based Knudsen number is less than 0.001 and 0.0001 for altitudes of 80 km and 60 km, respectively, and the use of a continuum approach is reasonable in this case. Note that ES-BGK computations was also conducted for an altitude of 80 km, and the solution was found to be nearly identical to the Navier-Stokes result (although it took orders of magnitude longer to use ES-BGK due to fairly slow convergence of the flow in the wake region) CFD++ is an unstructured parallel Reynolds Averaged Navier-Stokes code. It uses a fully implicit, 2nd order in space, 2nd order in time, Harten, Lax, van Leer, Contact discontinuity Riemann approximation algorithm. In the present axisymmetric computations, a single-block grid with a total of about 250,000 nodes is used. The density-velocity inflow / pressure outflow boundary conditions are used at the boundaries of the computational domain, and an isothermal, 2nd order slip, boundary condition with the wall temperature equal to the free stream value

is set at the space vehicle's surface.

RADIOMETRIC VANE ON A SINGLE VANE IN A MOVING FLOW

The first series of computations is performed for a single, stand-alone vane in a setup that approximates the conditions in the boundary layer near a space vehicle at 80 km. The gas is nitrogen, the vane is assumed to be circular with a diameter of 4 cm. The diameter is approximately ten times larger than the gas mean free path, so that the radiometric force is expected to be near its maximum. The free stream temperature and density are 214 and 1.4×10^{-5} kg/m^3, respectively, and the vane sides are kept at 214 K (wind side) and 244 K. The free stream velocity changes from 1 m/s to 3 m/s to 10 m/s in order to estimate the ability of the vane to compensate for a certain level of free stream velocity.

The results of the computations for the three free stream velocities under consideration are presented in Fig. 2. Note that only a quarter of the computational domain is shown here to better illustrate the flow in the vicinity of the nozzle. Here and below, the lower boundary is the symmetry axis, and the flow velocity is from left to right. Since the radiometric force is always directed from hot to cold, so that the cold surface of the vane advances and the hot surface recedes, the wind compensation purpose of the vane requires the temperature gradient across the vane be in the direction of the flow. As shown in Fig. 2 (left), the flow velocity does not have a noticeable effect of the distribution of gas temperature, which reaches over 238 K at the hot (right) side, and less than 216 K at the cold side for all three cases. Not only the fairly small (less than 0.001) Knudsen number reduces the temperature jump to about ! K, but it also results in very small, mostly less than 0.3 m/s, values of the flow velocity along the working (vertical) sides of the vane. The effect of flow velocity on the total radiometric force is therefore expected to be rather small.

Another property that changes with flow velocity is pressure, which is important from the point of view of the total radiometric force produced by the vane. For a 10 m/s flow, the gas pressure is visibly higher at the cold wall. Note that the pressure difference between the cold and hot sides of the vane is relatively small even for 10 m/s, amounting to less than 2% of the total gas pressure, but this difference is very important in terms of radiometric force, which typically does not exceed 0.5% of the gas pressure force on either cold or hot surface of the vane. For the 3 m/s case, the pressure at the hot side is much closer, but still lower, than the pressure at the cold side. Only for the smallest considered flow velocity of 1 m/s, the pressure at the hot side is clearly higher, and thus wind compensation may be possible.

The total pressure force on the vane is -1.5e-5 N, 1.13e-5 N, and 1.00e-4 N for 1, 3, and 10 m/s, respectively. Here, the positive value of the force corresponds to motion of the vane in the direction of the flow, and the negative force indicates the ability of a vane to compensate for a free stream velocity. Assuming the validity of the Stokes' law for a flow over a near-space vehicle, which appears reasonable since the flow is typically in the near-continuum or continuum flow regime, one may conclude that when the flow velocity in the boundary layer near a radiometer vane is about 1 m/s, the vane will compensate for a wind-related drag of a cross sectional area of the vehicle at least as large as the area of the vane (in this case, a cross sectional area of about 75 cm^2). Note here that the presence of a spacecraft surface will only increase the compensating ability of a radiometer, since the radiometric force was shown to increase [14] in the presence of a cold wall.

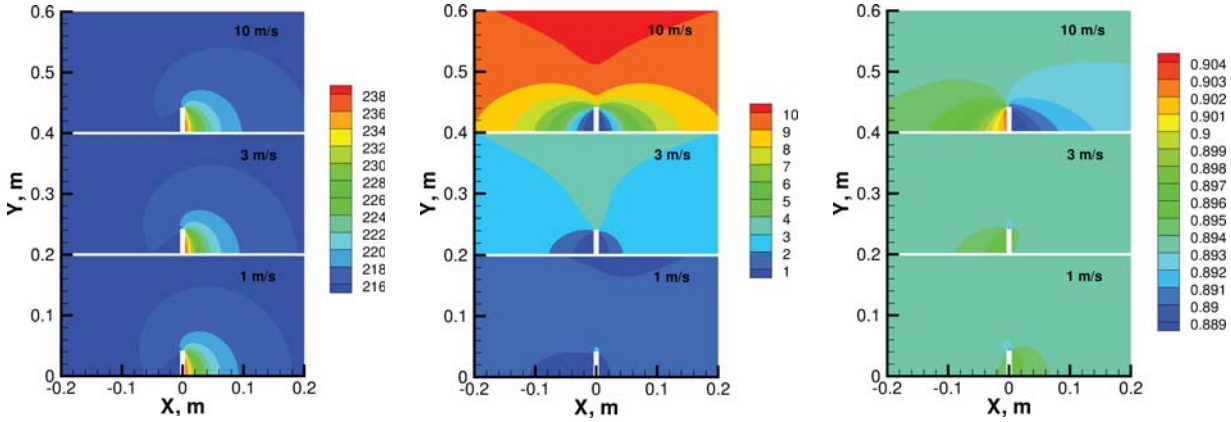

FIGURE 2. Gas properties over a single vane for different free stream velocities. Left: gas velocity (m/s) in X direction. Center: translational temperature (K). Right: pressure.

FLOW OVER A NEAR-SPACE VEHICLE

As shown in the previous section, a radiometer vane installed on a side of a near space vehicle is expected to compensate for a portion of the drag force resulting from a head wind when the gas velocity near the vane is at or smaller than 1 m/s. It is clear that while the total compensation capacity depends on the number of vanes in the radiometer array, the wind compensation efficiency of a single vane is primarily determined by the following factors: temperature gradient across the radiometer vanes, the strength of the head wind, and the geometry (length and thickness) of the near-space vehicle. In this work, the most unfavorable for the wind compensation conditions of a small (10 m long) spacecraft, high altitude (80 km), and high head winds (100 m/s) are considered, along with a more likely altitude of 60 km and a head wind of 30 m/s.

Comparison of flow velocities over an elliptic model of a small near-space vehicle is given in Fig. 3, where the results are normalized by their corresponding free stream values in order to simplify comparison between different cases. The actual computational domain spans from 0 to 50 m in the radial direction, and from -50 m to 50 m in the axial direction, and a close-in near the body is shown in Fig. 3 to show flow gradients in the boundary layer. For an altitude of 60 km, the boundary layer is relatively thin, and near the central part of the vehicle (X$\approx$ 0) it does not exceed 10% of the body thickness. Nevertheless, the small Knudsen number results in a significant decrease of velocities near the wall both in the front, where for the 100 m/s case they do not exceed approximately 2 m/s, and especially the rear part of the spacecraft, where they drop by over an order of magnitude compared to the front part. Of course, caution needs to be used when analyzing these numbers, since the Navier-Stokes solution is known to be incorrect in the Knudsen layer. For the 80 km cases, the velocities in the boundary layer are several times higher than the corresponding values for 60 km. Still, for the 30 m/s case they are less than 1 m/s for most part of the vehicle. The gas temperature, also shown in Fig. 3, changes only $\sim$ 1 K in the boundary layer for 80 km, 100 m/s, and even less than that for all other cases. This indicates that external temperature gradients will not play significant role for the radiometric force production, that will be governed by the temperature gradients across the vane.

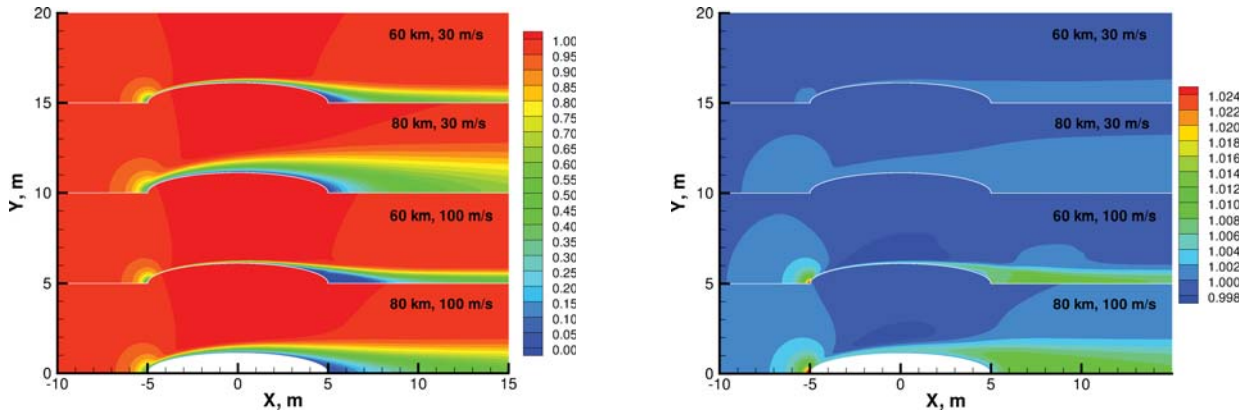

FIGURE 3. Flow properties over an elliptic profile for two altitudes and free stream velocities. Left: gas velocity (m/s) in X direction. Right: translational temperature (K). The properties are normalized by free stream values.

A more qualitative comparison of flow velocity in the boundary layer for the considered free stream conditions is presented in Fig. 4. The flow velocity has a small maximum observed at approximately 10 cm from the wall for the lower altitude, and 1 m from the wall for the higher altitude. In the boundary layer, the velocity decreases nearly linearly until the Knudsen layer. Note again that the Navier-Stokes solution is incorrect in the Knudsen layer, that propagates about a centimeter from the wall for 80 km, and less than a millimeter for 60 km. The inflow boundary conditions for the successive 2D ES-BGK simulations of a radiometer array, presented in the next section, are set at 1 cm for 60 km and 16 cm for 80 km, where the solution is essentially free of the Knudsen layer effects (they both are in the region of linear decrease of the flow velocity). The boundary conditions for the ES-BGK computations also included gas density and temperature (see Fig. 4, right), but the changes in these properties are minor (less than 0.5% from the free stream value for temperature and less than 1% for gas density), and the impact of these is therefore minimal.

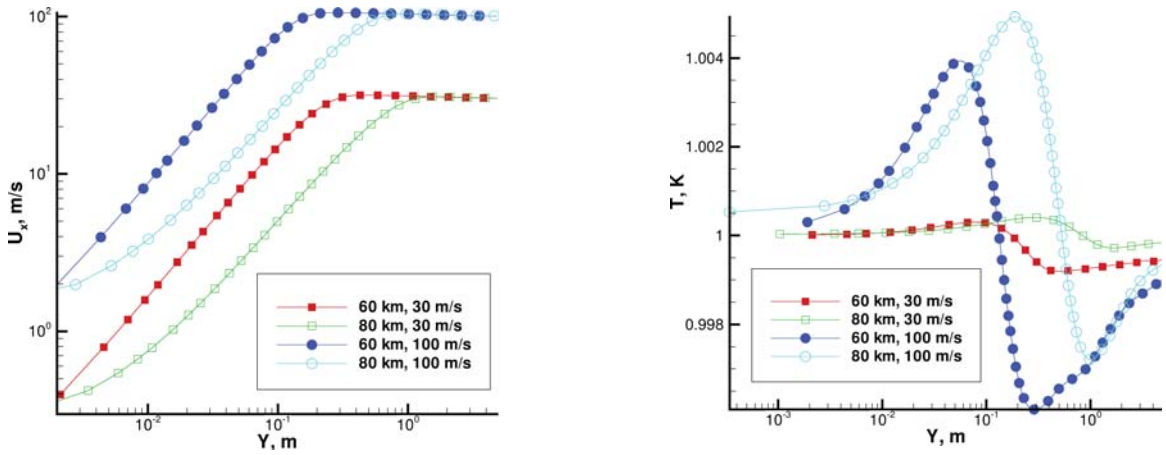

FIGURE 4. Flow velocity (left) and normalized temperature (right) in a cross section X=0. Y axis starts at the surface.

EFFICIENCY OF RADIOMETER ARRAYS FOR DIFFERENT FLOW CONDITIONS

The Navier-Stokes solutions of a flow over an elliptic profile are used to specify the boundary conditions for the successive ES-BGK simulations of a flow in the vicinity of the radiometer array. In order to check the validity of such an approach, the first computations have been conducted for a no-vane flow, so the the ES-BGK domain is rectangular, with periodic boundary conditions in the direction of the flow (left and right), wall condition with the fully diffuse reflection at the lower boundary, and prescribed flow parameters from the corresponding Navier-Stokes simulation at the upper boundary. For both altitudes, the computational domain is approximately 40 mean free paths in the radial direction. Since radial coordinate of the radiometer array is about 1 m, which is much larger than the size of the radiometer vanes (at ten gas mean free paths in length, they are 2.5 mm and 4 cm for 60 and 80 km, respectively), a two-dimensional setup is used in the ES-BGK modeling. The temperature difference between the hot and cold sides of the vanes is assumed to be 10 K and 30 K for 60 and 80 km, respectively.

Comparison of the flow velocity profiles along the radial coordinate, obtained by different approaches, is presented in Fig. 5, left. The results are for a cross section at X=0 (the center of the vehicle), and Y axis originates at the wall. For 60 km, the NS and ES-BGK profiles are close to linear for the shown range of spatial coordinates, and the difference between the methods is negligible. This confirms that the impact of the axial symmetry used in the NS modeling in minimal. For 80 km, there is some difference between the solutions, primarily attributed to two effects: the flow dimensionality (2D in ES-BGK versus axisymmetric in NS) and the unphysical slip boundary condition in NS near the wall. The latter one is mostly visible in the vicinity of the wall. Note that for both altitudes, the ES-BGK flow velocity at the inflow boundary matches the NS value, which indicates that the size of the ES-BGK computational domain is adequate. The other flow parameters, such as density and temperature, change little in the boundary layer, and the ES-BGK and NS profiles differ by less than 0.1%.

The results of ES-BGK computations of the boundary layer over a radiometer array at an altitude of 80 km and two free stream velocities are given in Fig. 5 (right). Generally, the impact of the free stream velocity on gas temperature near the vane is relatively small, but noticeable. For the 30 m/s case, the temperature is larger near the hot side, and smaller at the cold side, as compared to the 100 m/s case. This may be expected to reduce the radiometric force, since the temperature gradients in the normal direction to the radiometer appear smaller for 30 m/s. However, as will be shown below, the increase of the gas pressure at the wind side as a result of higher flow velocity is more important than the temperature gradient effect. The cold temperature of the vehicle surface (lower boundary) significantly affects the temperature, and should increase pressure on the hot side, and thus the total radiometric force. The results also show that the vane separation (the separation between the vanes is roughly equal to the vane height) is not large enough to remove the vane interference, as the temperature at the cold side is clearly affected by the hot side of the next vane (compare Figs. 2, left, and 5, right). However, a smaller separation allows for more closely packed radiometer array, thus increasing its total wind disturbance compensation ability.

The results for the lower altitude are given in Fig. 6. The normalized flow velocity is somewhat smaller for the 100 m/s case, even though the velocity slip is was generally found to be proportional to the flow velocity for the no-vane case shown in Fig. 5, left. This may be an indication of a significant pressure redistribution near the vanes

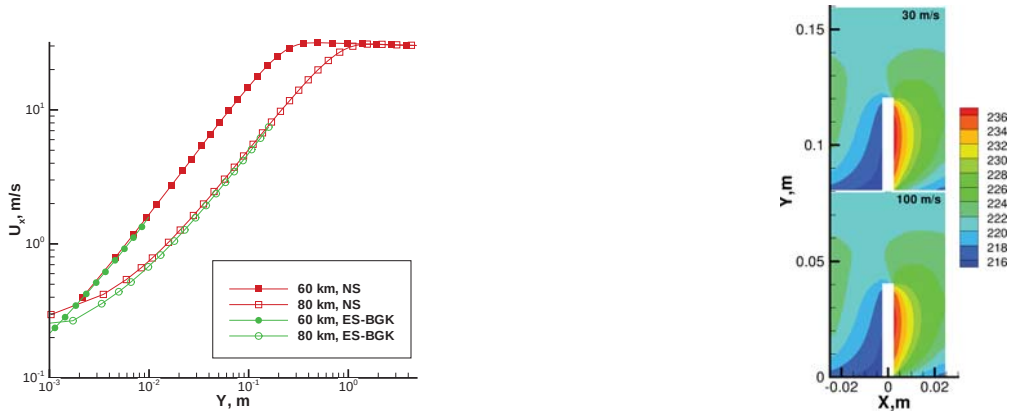

FIGURE 5. Left: velocity profiles in the boundary layer of a near-space vehicle obtained by two numerical methods. Right: translational temperature fields (K) over a vane at two free stream velocities.

from their hot to the cold sides when the flow velocity increases. This is illustrated in Fig. 6, right. The gas pressure is clearly higher near the hot side of the vane than near the cold side for the 30 m/s flow. The biggest pressure difference between the hot and cold sides is observed near the outer edge of the vane. For the 100 m/s case, a pressure maximum forms at the cold edge of the vane, obviously as a result of a stronger interaction between the moving gas and the vane.

FIGURE 6. Flow velocity normalized by the free stream value (left) and gas pressure (right) for two free stream conditions at an altitude of 60 km.

The results of the impact of flow conditions on the radiometric force production are summarized in Table 1. The values are given a force per length for a single radiometer row. Here again, a negative force value shows that the radiometric force acts in the direction opposite to the free stream, and thus indicates the ability of a vane to compensate for the wind disturbance. Negative force means that the radiometers move the vehicle in the direction of the drag. The main conclusion that can be drawn from the table is that for a head wind of 30 m/s, the radiometers are capable of generating a significant wind compensating force. As can be expected, the radiometers are generally less effective at a higher altitude, and at 80 km the vane is producing an about 30% lower force per degree K of the temperature difference between the vane sides than the comparable radiometer at 60 km (remember also that the vane size is 15 times larger at 80 km).

When the free stream velocity is increased to 100 m/s, the vanes can no longer compensate for the wind related drag. For an altitude of 60 km, the total force generated by a radiometer vane is close to zero (within the numerical error), thus indicating that for that altitude, radiometers can be used to compensate (totally or partially) for the wind force for wind velocities smaller than 100 m/s. For 80 km, the radiometer will in fact generate a significant force in the direction of the wind, as the force due to the finite flow velocity in the boundary layer is much bigger than the radiometric force due to the temperature gradient across the vane. Note that the force is smaller when the radiometer

TABLE 1.

Altitude, km	u, m/s	Location, m	Force, N/m
60	30	0	$-3.7\cdot10^{-5}$
60	100	0	$2\cdot10^{-7}$
80	30	0	$-7.6\cdot10^{-5}$
80	100	0	$1.3\cdot10^{-4}$
80	100	2.5	$4.7\cdot10^{-5}$

array is moved from the center of the vehicle halfway toward the rear (X=2.5 m), but positive. For 80 km, therefore, a radiometer array can only compensate for winds about 30 m/s or weaker.

CONCLUSIONS

Numerical analysis is presented of the feasibility of using radiometer arrays for wind drag compensation of near-space vehicles. The modeling includes a stand-alone vane immersed in a moving flow, and a radiometer array installed on a side of a model near-space vehicle. The first configuration is studied with an ES-BGK model kinetic equation solver, applied to an 80 km (Kn=0.1) flow with free stream velocities ranging from 1 to 10 m/s. A combined Navier-Stokes / ES BGK approach is used to examine the second configuration. Two altitudes, 60 and 80 km, and two free stream velocities, 30 m/s and 100 m/s, were considered. The temperature difference across the radiometer vane was 10 and 30 K.

It has been shown that a stand-alone vane can compensate for a drag on a body with a comparable cross sectional area, caused by free stream velocities on the order of 1 m/s (Mach numbers on the order of 0.001). For near-space vehicles, the use of radiometers for wind disturbance compensation appears reasonable when wind velocities do not exceed approximately 30 m/s, although higher velocities may be possible for altitudes of 60 km and smaller.

ACKNOWLEDGMENTS

The authors wish to acknowledge the support of the Advanced Concepts Group of the Air Force Research Laboratory's Propulsion Directorate, Edwards AFB, CA.

REFERENCES

1. Fresnel A (1825) Note sur la repulsion que des corps échauffés execent sur les autres à des distances sensibles. Annales de Chimie et de Physique 29:57-62
2. Crookes W (1874) On attraction and repulsion resulting from radiation. Phil. Trans. R. Soc. of London 164:501-527
3. Reynolds O (1879) On Certain Dimensional Properties of Matter in the Gaseous State. Phil. Trans. R. Soc. of London 170:727-845
4. Maxwell JC (1879) On stresses in rarified gases arising from inequalities of temperature. Phil. Trans. R. Soc. of London 170:231-256
5. Einstein A (1924) Zur theorie der radiometrerkrafte. *Zeitschrift fur Physik* 27:1-5
6. Binning G, Quate CF, Gerber CH (1986) Atomic force microscope. Physical Review Letters. 56:930-933
7. Wadsworth DC, Muntz EP (1996) A computational study of radiometric phenomena for powering microactuators with unlimited displacements and large available forces. J. Microelectromech. Syst. 5(1):59-65
8. Passian A, Wig A, Meriaudeau F, Ferrell TL, Thundat T. (2002) Knudsen forces on microcantilevers. J. Appl. Phys. 92(10):6326-6333
9. Passian A, Warmack RJ, Ferrell TL, Thundat T (2003) Thermal Transpiration at the Microscale: A Crookes Cantilever. Phys. Rev. Lett. 90(12):124503
10. Benford G., Benford J. (2005) An aero-spacecraft for the far upper atmosphere supported by microwaves. Acta Austonautica 56:529-535
11. B. Cornella, A. Ketsdever, N. Gimelshein, S. Gimelshein, To appear in J. Propulsion and Power, 2012.
12. L. Mieussens, "Discrete-Velocity Models and Numerical Schemes for the Boltzmann-BGK Equation in Plane and Axisymmetric Geometries," *Journal of Computational Physics*, 2000, Vol. 162, pp. 429-466.

13. D. C. Wadsworth, N.E. Gimelshein, S. F. Gimelshein, I.J. Wysong, "Assessment of Translational Anisotropy in Rarefied Flows Using Kinetic Approaches," *Proc. XXVI Int. Symp. on Rarefied Gas Dynamics*, Kyoto, Japan, July 2008.
14. N. Selden, C. Ngalande, N. Gimelshein, S. Gimelshein and A. Ketsdever, Origins of radiometric forces on a circular vane with a temperature gradient, Journal of Fluid Mechanics, Vol. 634, September 2009, pp 419-431.
15. Chakravarthy S. and Peroomian O. Some internal flow applications of a unified-grid CFD methodology, AIAA Paper 96-2926.